Cell Reports

Supplemental Information

Direct In Vivo Manipulation and Imaging of Calcium Transients in Neutrophils Identify a Critical Role for Leading-Edge Calcium Flux

Rebecca W. Beerman, Molly A. Matty, Gina G. Au, Loren L. Looger, Kingshuk Roy Choudhury, Philipp J. Keller, and David M. Tobin

Supplemental Figures

Figure S1

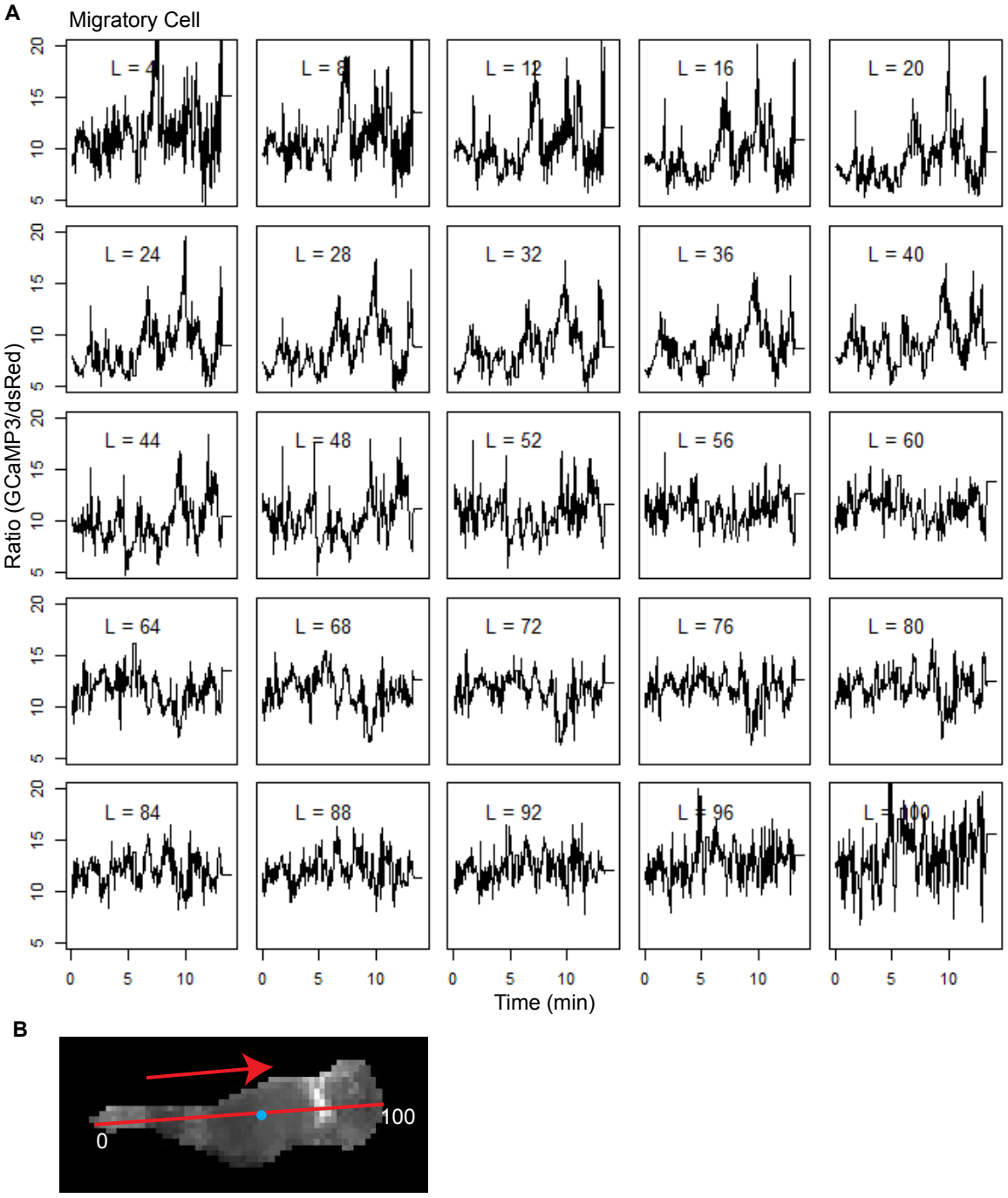

Figure S1 (Relates to Figure 1). Calcium activity profiles from a migrating neutrophil.
(A) The migrating cell was sectioned into 25 parts across its length (1-100 units), such that L=4 (the upper left hand box) displays the average GCaMP3/dsRed signal (y axis) across time (x axis,

minutes) within the lagging edge of the cell and L=100 corresponds to the leading edge of the migrating cell. This profile corresponds to the cell images in Figure 1.
(B) Example of defining cell length at time *t* for ratiometric quantitation described in the Supplemental Experimental Procedures. The red arrow indicates the direction of motion, passing through the centroid of the cell (blue circle). The back of the cell is distance $d = 0$ on the line and front of the cell is $d = 100$. Calcium expression from all points in the cell is mapped to the nearest point on the line.

Figure S2

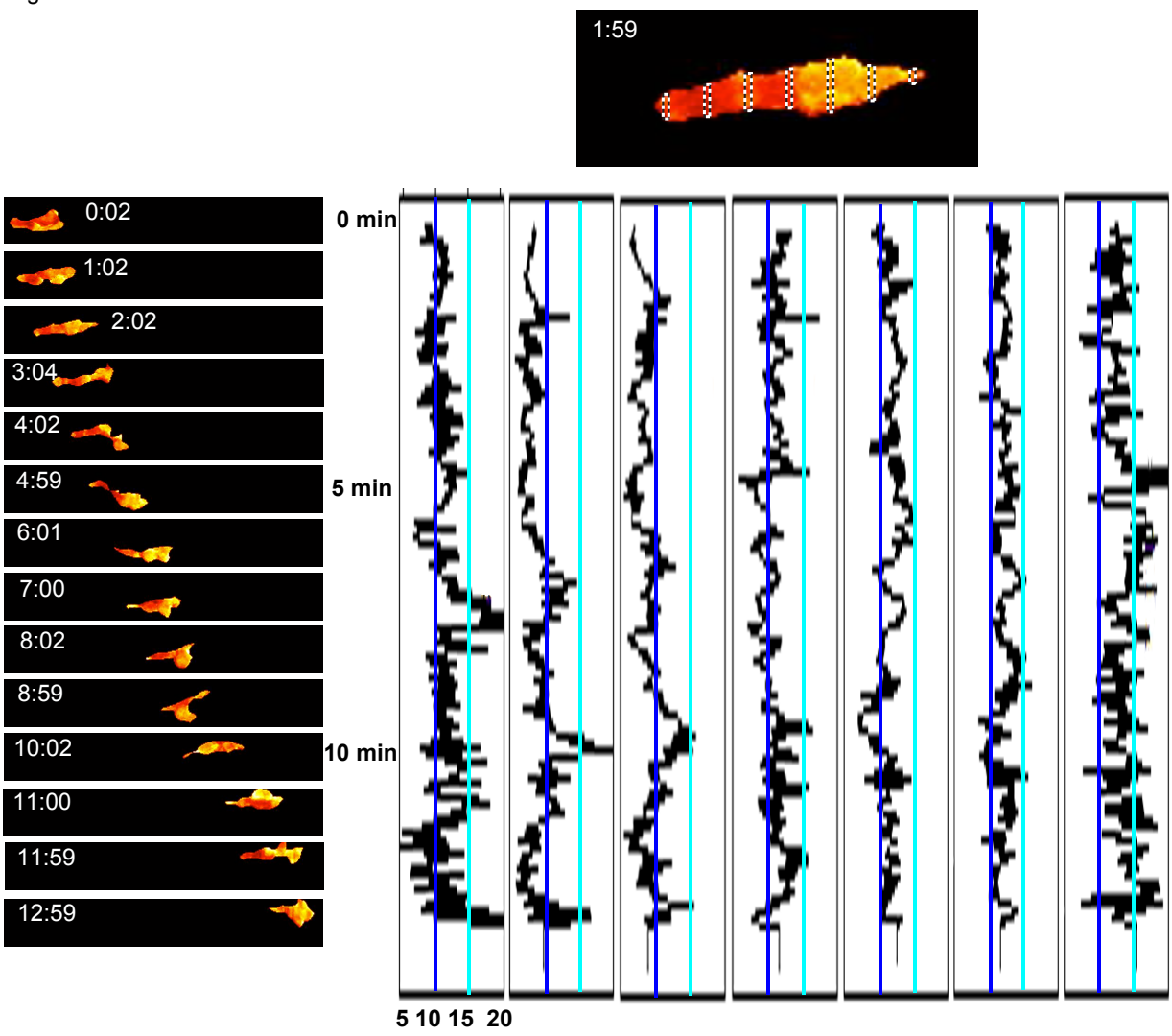

Figure S2 (Relates to Figure 1). Detailed analysis of calcium activity profile from a migrating neutrophil.

The top image of a cell illustrates how the boxes L=4, 20, 36, 52, 68, 84, and 100 from Figure S1 were rotated, stretched, and magnified to highlight the enriched calcium flux at the leading edge, and to a lesser extent the lagging edge over time. The y axis is time (min) and the x axis is the GCaMP3/dsRed ratio oriented such that the turquoise line shows a visual threshold of the ratio at 15 and the dark-blue line shows a visual threshold of the ratio at 10. The time-lapse ratiometric cell images on the left correspond approximately to the time axis on the calcium activity profiles to provide a visual readout of the quantified signal graphed adjacently.

Figure S3

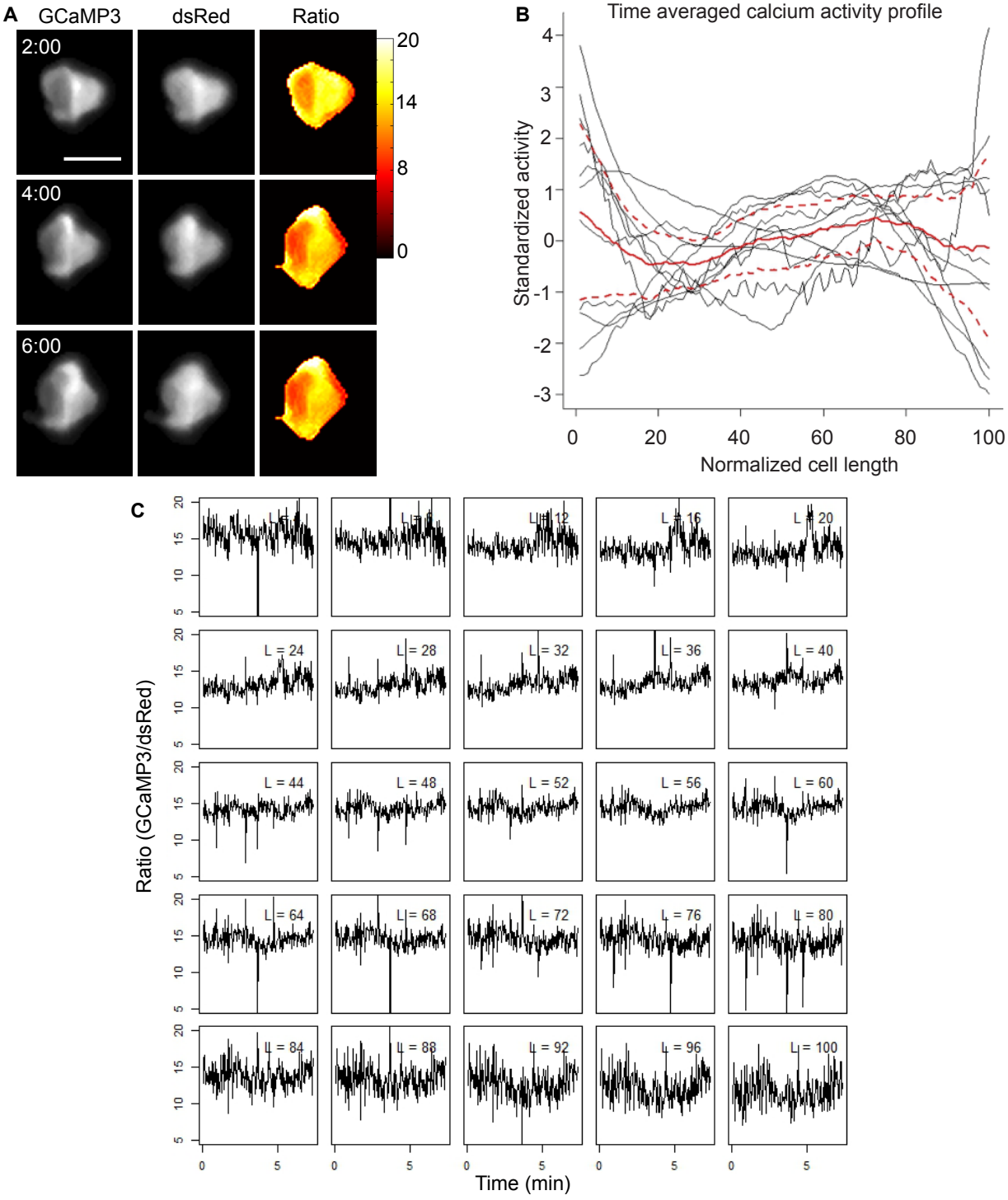

Figure S3 (Relates to Figure 1). Stationary neutrophils do not exhibit a distinguishable pattern of calcium localization.

(A) Still frames from time-lapse microscopy show a stationary neutrophil in a *Tg(LysC:GCaMP3; LysC:dsRed)* larva after a caudal fin wound. Each channel was captured

sequentially (GCaMP3 or dsRed) and the resulting ratiometric image is GCaMP3/dsRed. t=0 corresponds to approximately 40 min post wounding. The scale bar is 10μm.
(B) Summary graph displays the time-averaged calcium activity profile across the length of a stationary neutrophil (normalized to 100 units at each frame; 0 is edge most distal to wound and 100 is edge most proximal to the wound). Each individual neutrophil is graphed in black (n=11 from 5 animals) with the average profile outlined in red and bound by the 95% confidence intervals (dashed red lines).
(C) Calcium activity profiles from stationary neutrophil in (A). The stationary cell was sectioned into 25 parts across its length (1-100 units), such that L=4 (the upper left hand box) displays the average GCaMP3/dsRed signal (y axis) across time (x axis, minutes) within the left-most (distal to wound) edge of the cell and L=100 corresponds to the right-most (proximal to wound) edge of the stationary cell.

Figure S4

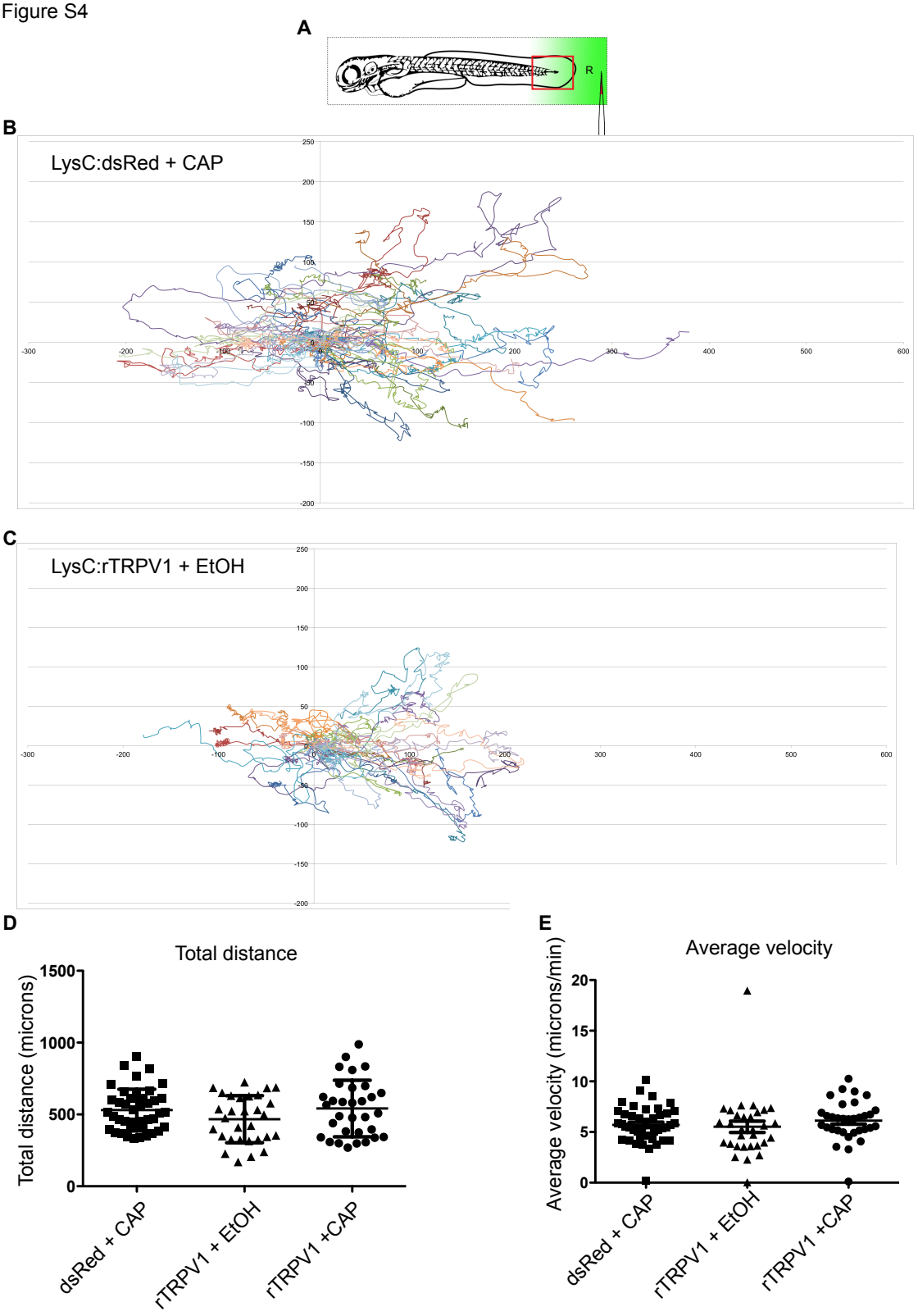
A
R
B
LysC:dsRed + CAP
C
LysC:rTRPV1 + EtOH
D
Total distance
Total distance (microns)
1500
1000
500
0
dsRed + CAP
rTRPV1 + EtOH
rTRPV1 +CAP
E
Average velocity
Average velocity (microns/min)
20
15
10
5
0
dsRed + CAP
rTRPV1 + EtOH
rTRPV1 +CAP

Figure S4 (Relates to Figure 4). Neither low-dose capsaicin gradient alone nor rTRPV1 transgene alone is sufficient to alter neutrophil migratory behavior.

(A) Cartoon depicting larval orientation. The red box approximates where the tracks on the graph below would superimpose onto the larvae analyzed in Figure 4 and Figure S4.

(B,C) (x,y) coordinates for each neutrophil at every time-point tracked. The track for each cell was normalized such that the starting (x,y) position was (0,0) for every cell. The unit of measurement on the axes is microns.

(D,E) Graphs show no difference in the average distance (D) or average velocity (E) for tracked neutrophils amongst all three experimental groups. Error bars are mean ± s.d. (D) and mean ± s.e.m (E).

Supplemental Movie Legends

Movie S1 (Relates to Figures 1A and S3A). Excerpts from ratiometric time-lapse of migrating neutrophil (Part 1) and stationary neutrophil (Part 2).
Tg(LysC:GCaMP3; LysC:dsRed) larvae after caudal fin amputation. Colorimetric scale is the same as referenced figures.

Movie S2 (Relates to Figures 2A and 2C). Excerpts from time-lapse of neutrophils migrating toward a ventral fin wound in *Tg(LysC:GCaMP3)* larva (Part 1) and calcium flashes upon neutrophil phagocytosis of *P.aeruginosa-mCherry* in *Tg(LysC:GCaMP3)* larvae (Parts 2-4).
There is a pause for manual re-focusing between 20:20 and 20:35 in Part 1. Parts 2-4: There are three different examples of phagocytosis, Parts 2 and 3 follow different neutrophils within the same animal and Part 4 follows a neutrophil within a different animal.

Movie S3 (Relates to Figure 3A). Time-lapse microscopy shows GCaMP3 fluorescence in control *Tg(LysC:dsRed; LysC:GCaMP3)* larva (Part 1) and *Tg(LysC:rTRPV1; LysC:GCaMP3)* larva (Part 2) after addition of capsaicin.

Movie S4 (Relates to Figure 4). Part 1 shows a *Tg(LysC:rTRPV1; LysC:GCaMP3)* larva embedded in agarose after exposure to a high-dose capsaicin gradient and Parts 2-5 show neutrophil migratory responses to low-dose capsaicin and vehicle gradients.
(Part 1) The time-lapse shows GCaMP3 fluorescence increasing in a caudal to rostral pattern after injecting a high-dose of capsaicin into the agarose proximal to the caudal fin (right-hand side). (Parts 2-5) Examples of neutrophil tracking with the following strains and conditions (real-time duration for each time-lapse was 1.5 hr): *Tg(LysC:dsRed; LysC:GCaMP3)* (Part 2) and *Tg(LysC:rTRPV1; LysC:GCaMP3)* (Parts 4,5) were treated with low-dose capsaicin gradients and *Tg(LysC:rTRPV1; LysC:GCaMP3)* (Part 3) was treated with an ethanol gradient. R designates the reference point closest to the gradient focal point. Part 5 depicts neutrophil migration in an *Tg(LysC:dsRed; LysC:GCaMP3)* animal with a ventrally located capsaicin gradient, reference point (R).

Movie S5 (Relates to Figure 5). Neutrophil motility in amputated larvae under control or SKF 96365 treatment.
Time-lapse shows GFP fluorescence with a representative *Tg(LysC:GFP)* larva treated with DMSO-vehicle control water (top) or 20μM SKF 96365 (bottom) after caudal fin amputation. Each neutrophil track is a different color, the white dashed line approximately indicates the amputation, and the real-time duration for each time-lapse was 1 hr.

Supplemental Experimental Procedures

Zebrafish strains. All zebrafish husbandry and experimental protocols were performed in compliance with policies approved by the Duke University Institutional Animal Care and Use Committee. The transgenic lines *Tg(LysC:GCaMP3^{xt1})* and *Tg(LysC:rTRPV1-tdTomato^{xt4})*, were made by injecting transposase mRNA (25ng/µl) (from p3T3, transcribed with MEGAscript T3 kit, Life Technologies) and Tol2 containing DNA constructs (50ng/µl) into single cell embryos (background, *AB). The constructs were assembled with Tol2kit reagents and Gateway Cloning methods (Life Technologies) (Kwan et al., 2007). The 5' *LysC* promoter element has been previously described (Hall et al., 2007; Oehlers et al., 2015). The middle elements were generated via PCR amplification of plasmids containing GCaMP3 (Tian et al., 2009) or rat TRPV1 (rTRPV1) (Grandl et al., 2010) using primers containing attB1 and attB2 sites and recombining into pDONR 221, and the 3' elements were tdTomato (for rTRPV1 construct) or SV40polA (for GCaMP3 construct) in pDONR P2R-P3. The destination vector was pDestTol2pA2. *Tg(LysC:dsRed^{nz50})* and *Tg(LysC:GFP^{nz117})* have been described elsewhere (Hall et al., 2007).

Time-lapse imaging. All solutions used with live embryos were diluted in filtered fish water (from Aquaneering fish system, pH, electrolyte balanced). Embryos were cleaned in 0.5% hypochlorite solution (Fisher SS290), and transferred to phenylthiourea (PTU) (0.03g/L final concentration) at 24hpf to facilitate fluorescence imaging by preventing pigmentation. *Tg(LysC:GCaMP3)* larvae were imaged at 2 days post fertilization (dpf) for bacterial infection experiments and all other transgenic larvae were imaged at 3 dpf. For microscopy, larvae were anesthetized in 0.016% Tricaine (MS-222) and immobilized in 1% low melting point agarose (Fisher BP165) and imaged through no. 1.5 coverslip in the bottom of a 35mm petri dish (MatTek) on an inverted Zeiss axio observer Z1 (20x objective, 0.645 µm/pixel) or inverted Nikon TE-2000U (20x objective, 0.32µm/pixel). Phagocytosis was captured by caudal artery injection of bacteria and immediate imaging in agarose. Ventral fin wounding and caudal tail wounds were carried out with a sterile no. 11 miltex razor in tricaine anesthetized larvae and imaged immediately or several hours post wounding as determined by the experiment.

Light-sheet fluorescence microscopy experiments were carried out with a SiMView microscope using specimens embedded in 1.0% low melting point agarose and immobilized with 0.016% tricaine (Tomer et al., 2012). Fluorescence was detected with Nikon 16x detection objectives and Orca Flash 4.0 sCMOS cameras (Hamamatsu), providing a lateral pixel size of 0.41 µm. Three-dimensional image stacks were recorded for a ~50 µm deep volume, using piezo-stepping of the detection objective and galvanometer scanning of the light sheet with a z-spacing of 5.0 µm (Ahrens et al., 2013). Two-color imaging was performed by rapid, sequential acquisition of GCaMP3 and tdTomato channels, using a temporal sampling of 2 seconds for the entire imaging volume and both color channels.

Infections/bacterial preparations. *Pseudomonas aeruginosa* (PAO1) carrying a constitutively expressed *mCherry* or *GFP* plasmid was grown in LB media or LB agar plates supplemented with carbenicillin (200µg/ml) as previously described in (Brannon et al., 2009). Briefly, PAO1 cultures were grown to an OD_{600} of 0.6-0.8 before injecting approximately 50-100 CFU into the hindbrains or caudal artery (with trace amount of phenol red to follow injection). Approximate

CFU for injected bacteria was counted by carrying out an identical injection directly onto agar plates supplemented with the appropriate antibiotic.

Quantification of calcium flashes and ratiometric analyses. Light-sheet microscopy images were analyzed using maximum projections with background fluorescence subtracted. The signal in the green channel was multiplied by a constant factor to generate a positive ratio for the GCaMP3/dsRed ratiometric analysis. Individual cells were masked using the Imaris tracking function and subsequently setting all pixels outside the mask to zero for both the red and green fluorescent channels before undergoing additional analyses as detailed below.

Quantification of calcium profiles.

Quantification of the intra-cellular calcium distribution is complicated by the fact that the cell changes shape over time. This makes it difficult to identify a 'back' and a 'front' for the cell. We use the path of the cell over time to identify the direction of motion and the orientation of the cell. The path of the cell is estimated as $c(t) = \left(c_x(t), c_y(t)\right)$, where $c(t)$ is the centroid of the cell at time t. The orientation of the cell is estimated as $\theta(t) = \arctan\left(\partial/\partial t\, c(t)\right)$, i.e. the direction of the tangent to the motion path at time t. Calcium expression within the cell at time t, $C(t)$, is quantified by the ratio image $R(t) = \left(R(x,y) : x,y \in C(t)\right)$. The two-dimensional expression $R(t)$ is mapped to a line running through the centroid of the cell $c(t)$, in the orientation $\theta(t)$ by mapping points (x,y) within the cell $C(t)$, using the formula

$$R(d,t) = \sum_{\{P_\theta(x,y)=d : (x,y)\in C(t)\}} R(x,y) \qquad (1.1)$$

Where P_θ is the projection matrix mapping points (x,y) to the aforementioned line. We normalize the distance d along the line to be 0 at the rear of the cell and 100 at the front of the cell (Figure S1B).

The calcium expression profile $R(d,t)$ can be visualized in time (Figure S1) or space (Figure 1C). For Figure 1C, we calculate a time-averaged spatial profile: $\bar{R}(d) = T^{-1}\sum_{t=1}^{T} R(d,t)$, where T is the number of time points imaged. The advantage of this quantification is that it allows us to map the calcium expression of cells of different shapes and sizes, which were observed for different lengths of time, to a common spatial co-ordinate system (Figure 1C). The calcium expression of each cell is a 1-d curve, which can then be averaged across cells as: $\bar{\bar{R}}(d) = n^{-1}\sum_{i=1}^{n} \bar{R}_i(d)$, where $\bar{R}_i(d)$ is the spatial profile of the i-th cell. Similarly, we can quantify inter-cell variation by calculating the standard deviation across cells as: $SD_R(d) = \sqrt{(n-1)^{-1}\sum_{i=1}^{n}\left(\bar{R}_i(d) - \bar{\bar{R}}(d)\right)^2}$. These means and SDs can then be used to construct a pointwise 95% confidence band for the average spatial profile as:

$$95\%\ \text{C.I.}: \quad \bar{\bar{R}}(d) \pm 1.96\frac{SD_R(d)}{\sqrt{n}} \qquad (1.2)$$

Quadratic modelling and inference of profile shapes.

For a more descriptive comparison, we fit a quadratic model to the average calcium activity profiles, of the form:

$$R_i(d) = a_j + b_j(d-50) + c_j(d-50)^2 + \varepsilon_j(d) \quad (1.1)$$

Where $R_i(d)$ is the average calcium profile for cell i at a position d along the length of the cell (l = 0 is rear and l = 100 is front). The coefficient, a_j denotes the mean value of the profile at the middle of the cell (d = 50), b_j denotes the trend of the profile along the length of the cell and c_j denotes the curvature of the profile. A positive curvature implies a convex curve (like a cup) while a negative curvature implies a concave curve (like an arch), while 0 curvature implies a linear curve. The quadratic model appears to fit a number of the profiles quite well, which is reflected in median R^2 values above 80% for both stationary and mobile cells. We analyzed the estimated curvature values separately for mobile and stationary cells. For mobile cells, the mean curvature across all cells was 1.55, with a 95% confidence interval of (0.98, 2.13). The null hypothesis of the mean curvature for mobile cells being 0 is rejected with a p-value = 0.00006 using a one sample t-test. For stationary cells, the mean curvature across all cells was -0.02, with a 95% confidence interval of (-1.43, 1.40). The null hypothesis of the mean curvature for stationary cells being 0 cannot be rejected with a p-value = 0.98 using a one sample t-test. We can thus conclude that the average spatial profile of calcium expression of a mobile neutrophil cell has a convex shape, i.e. elevated at the front and rear and lowest in the middle. For stationary cells, since there is no preferred direction of motion, the average spatial profile of calcium expression is approximately constant all through the cell.

For Figure 1D, cells were demarcated by mapping all points within the cell, using a standardized scale of 0 to 100 for the cell length, with 0 being the lagging edge and 100 being the leading edge, along the principal axis of the cell's motion. The average activity of all these points, with a length greater than 80, was averaged across all time points, and then calculated to get the average activity for the leading one-fifth of the cell. The average activity for the lagging one-fifth of the cell was analogously calculated. These two numbers were differenced within each cell to yield the distribution in the box plot. We tested the hypothesis that the average difference was positive using a one sample t-test. This analysis was also repeated using one-third of the leading and lagging edges as well.

Whole-cell calcium flashes from ventral wounded 3dpf *Tg(LysC:GCaMP3)* larvae were quantified by manually scoring cells that displayed an obvious increase in green fluorescence during the time-lapse session. The number of flashes for each cell was then divided by the total time the cell was observed. Whole-cell calcium flashes associated with phagocytosis in *Tg(LysC:GCaMP3)* larvae were assessed by analyzing multiple imaging sessions, counting phagocytosis as occurring if the bacteria became trapped and moved with the immune cell in subsequent frames.

Capsaicin treatments and measured calcium flux response. 10mM capsaicin (Sigma) stock was made in ethanol and stored at 4°C and fresh dilutions were prepared for each experiment such that the final ethanol concentration was 1.4% to help maintain solubility; the final capsaicin concentration was 20µM. To record and measure calcium flux in *Tg(LysC:rTRPV1)* animals after treatment with capsaicin, anesthetized larvae were mounted in ~50-100µl 1% low-melt

agarose, followed by addition of 3ml of 20µM capsaicin before starting the multi-position time-lapse sessions as quickly as possible. To measure the change in GCaMP3 fluorescence over time (Figure 2 and Figure 3), the fluorescence intensity for each neutrophil was quantified by measuring the mean fluorescence intensity within a region of interest (ROI) that fit inside the neutrophil being tracked. The background fluorescence was subtracted from each mean ROI measurement (F) at each timepoint and at the first frame of the time lapse (F0). For Figure 3, a few of the time points for the *Tg(LysC:rTRPV1)* were averaged from fewer than 5 cells because some cells went out of focus or migrated out of the field of view during the time-lapse.

For wounding/PAO1 infection experiments, larvae were subjected to treatment with vehicle alone (1.4% ethanol) or repeated 10 min pulses in 20µM capsaicin, followed by 30 min recovery sessions in 1.4% ethanol for up to 2 hr post wounding or post hindbrain injections with PAO1. Capsaicin pulsing was chosen to maximize the amount of time the neutrophils would experience high intracellular calcium levels before channel desensitization or induction of cell death. To control for capsaicin-mediated cell death during extended periods of calcium influx, one group of *Tg(LysC:rTRPV1)* larvae was pulsed with 20µM capsaicin for 2 hours before caudal fin wounding and then soaked in 1.4% ethanol for 2 hr before quantification of neutrophil recruitment to the caudal wound. Quantification of neutrophil recruitment was carried out in anesthetized larvae by counting the number of fluorescent neutrophils within 100µm of the caudal fin wound or within the hindbrain ventricle.

Generating capsaicin gradient and subsequent quantification of cell movement. Anesthetized 3dpf larvae were mounted in MatTek dishes in 100µl of 1% low-melt agarose as described previously and arranged in parallel to each other. The injection needle was placed approximately 500µm away from the most distal point of the mounted larvae such that the needle would go into the agarose, but not touch the bottom of the MatTek dish (see Figure 4A). Approximately 0.5µl of low-dose capsaicin (100µM) or high-dose capsaicin (1mM, only used in Movie S4 part 1 for proof of principle) (in 1.4% ethanol and phenol red to visually track the injection) was injected into a straight line perpendicular to the mounted larvae (with the exception of Movie S4 part 5 in which capsaicin was injected in parallel with the mounted larva). After capsaicin injection, the larvae were immediately imaged using time-lapse fluorescent microscopy, as previously described in "Capsaicin treatments and measured calcium flux response," but with no additional liquid media added on top of the agarose. The larvae were imaged with a 5x objective (2.58µm per pixel), approximately every 10 seconds for 1.5 hours, with z resolution set to 15-20µm per section, for 50-120µm total as dictated by larval mounting conditions.

Each larva was carefully inspected for any tissue tearing or wounds from a brightfield z-stack taken before each time-lapse, and eliminated from quantification if they were found to carry any wounds. Cells were manually tracked from maximum-projections of time-lapses (tracking every 5th frame, or every 50-60sec) using MTrackJ (ImageJ). For each animal, a reference point, R, was selected outside of the caudal fin to approximate the center of the injected gradient. Cells were selected for tracking if they displayed motility and were located proximal to the caudal fin. "Distance traveled toward R" (D2R) was calculated by subtracting the final distance to R from the initial distance to R for each tracked cell. "Straightness ratio" was calculated by dividing the final D2S (Euclidean distance from start point to current point) by the final Len (total length traveled), such that "1" indicates the cell traveled in a straight line and a straightness ratio closer to "0" indicates a more circuitous, meandering route. "Total distance"

(Len) was calculated by MTrackJ as the total length traveled. “Average velocity” (average v) was calculated by MTrackJ.

SKF 96365 treatments and analyses. 10mM SKF 96365 (Cayman Chemical) stock was made freshly in DMSO for each experiment with 1mg aliquots. The final working concentration was 20μM SKF 96365 in 0.5% DMSO in fish water and the control solution was 0.5% DMSO in fish water. Experiments were carried out at 3dpf using either *Tg(LysC:dsRed)* or *Tg(LysC:GFP)* for each experiment. Fin amputation, neutrophil quantification, and time-lapse experiments with control or SKF 96365 treatments were carried out similarly to those described for “Capsaicin treatments and measured calcium flux response,” except that treatments were constant (no pulsing), and neutrophil recruitment was measured 3 hours post wounding and the amputated larvae were imaged with a 5x objective (2.58μm per pixel), approximately every 30 seconds for 1hr, with a z-resolution of 48μm total. Tracking neutrophil migration patterns was carried out similarly to that described for “Generating capsaicin gradient and subsequent quantification of cell movement,” except that cells were tracked every 30 seconds in this group of experiments.

Supplemental References

Ahrens, M.B., Orger, M.B., Robson, D.N., Li, J.M., and Keller, P.J. (2013). Whole-brain functional imaging at cellular resolution using light-sheet microscopy. Nat Methods *10*, 413-420.

Brannon, M.K., Davis, J.M., Mathias, J.R., Hall, C.J., Emerson, J.C., Crosier, P.S., Huttenlocher, A., Ramakrishnan, L., and Moskowitz, S.M. (2009). Pseudomonas aeruginosa Type III secretion system interacts with phagocytes to modulate systemic infection of zebrafish embryos. Cell Microbiol *11*, 755-768.

Grandl, J., Kim, S.E., Uzzell, V., Bursulaya, B., Petrus, M., Bandell, M., and Patapoutian, A. (2010). Temperature-induced opening of TRPV1 ion channel is stabilized by the pore domain. Nature neuroscience *13*, 708-714.

Hall, C., Flores, M.V., Storm, T., Crosier, K., and Crosier, P. (2007). The zebrafish lysozyme C promoter drives myeloid-specific expression in transgenic fish. BMC developmental biology *7*, 42.

Kwan, K.M., Fujimoto, E., Grabher, C., Mangum, B.D., Hardy, M.E., Campbell, D.S., Parant, J.M., Yost, H.J., Kanki, J.P., and Chien, C.B. (2007). The Tol2kit: a multisite gateway-based construction kit for Tol2 transposon transgenesis constructs. Dev Dyn *236*, 3088-3099.

Oehlers, S.H., Cronan, M.R., Scott, N.R., Thomas, M.I., Okuda, K.S., Walton, E.M., Beerman, R.W., Crosier, P.S., and Tobin, D.M. (2015). Interception of host angiogenic signalling limits mycobacterial growth. Nature *517*, 612-615.

Tian, L., Hires, S.A., Mao, T., Huber, D., Chiappe, M.E., Chalasani, S.H., Petreanu, L., Akerboom, J., McKinney, S.A., Schreiter, E.R.*, et al.* (2009). Imaging neural activity in worms, flies and mice with improved GCaMP calcium indicators. Nat Methods *6*, 875-881.

Tomer, R., Khairy, K., Amat, F., and Keller, P.J. (2012). Quantitative high-speed imaging of entire developing embryos with simultaneous multiview light-sheet microscopy. Nat Methods *9*, 755-763.